Received April 27, 2020, accepted May 11, 2020, date of publication May 19, 2020, date of current version June 8, 2020.

Digital Object Identifier 10.1109/ACCESS.2020.2995552

Development of a Connected Vehicle Dynamic Freeway Variable Speed Controller

HOSSAM M. ABDELGHAFFAR[1,2], MAHA ELOUNI[1], YOUSSEF BICHIOU[1], AND HESHAM A. RAKHA[1,3], (Fellow, IEEE)

[1]Center for Sustainable Mobility, Virginia Tech Transportation Institute, Virginia Tech, Blacksburg, VA 24061, USA
[2]Department of Computer Engineering and Systems, Faculty of Engineering, Mansoura University, Mansoura 35516, Egypt
[3]The Charles E. Via, Jr. Department of Civil and Environmental Engineering, Virginia Tech, Blacksburg, VA 24061, USA

Corresponding author: Hesham A. Rakha (hrakha@vt.edu)

This work was supported in part by the Department of Energy through the Office of Energy Efficiency and Renewable Energy (EERE), Vehicle Technologies Office, Energy Efficient Mobility Systems Program, under Award DE-EE0008209, and in part by a gift from Toyota InfoTechnology.

ABSTRACT Traffic congestion is a major challenge in urban areas, and is associated with longer travel times, increased vehicle emissions, and numerous vehicle crashes. Creating an efficient mobility system is difficult, given that each driver is usually trying to optimize their individual trip within the network without accounting for other road users. However, new technologies in modern vehicles, especially connected vehicle technologies, make it increasingly possible to find solutions to network efficiency problems. Connected technologies allow data sharing between vehicles, allowing for greater system optimization. This work takes advantage of connectivity to develop a global framework to increase transportation network efficiency and address the aforementioned challenges. To enhance mobility, this paper presents a dynamic freeway speed controller based on the sliding mode theory, which uses the fundamental equations governing traffic dynamics in combination with variable speed limit control in order to provide advisory speeds for connected vehicles. Simulation results on a downtown Los Angeles network show significant reductions in trip times and delays both on freeways (where the control was activated) and network-wide (i.e., freeways and other roadways). Specifically, the results for the entire network showed a 12.17% reduction in travel time and a 20.67% reduction in total delay. These results had the secondary effect of reducing fuel consumption and therefore CO_2 emissions by 2.6% and 3.3%, respectively. The results for the freeway network alone showed a 20.48% reduction in travel time and a 21.63% reduction in queued vehicles. These results reveal the significant potential benefits of using the proposed speed harmonization controller on real large-scale networks.

INDEX TERMS Connected vehicles, large scale network, sliding control, speed harmonization, variable speed control.

I. INTRODUCTION

Highway congestion is a severe problem, causing delays, increased vehicle emissions, greater fuel consumption levels due to continual accelerations/decelerations [1], and numerous vehicle crashes as the result of sudden braking maneuvers when vehicles traveling at high speeds approach a queue. Various studies have tried to address this issue via speed harmonization (SH), an intelligent transportation system application. SH regulates vehicle velocities to improve traffic conditions, increase driver/passenger safety, and effectively reduce congestion, which reduces environmental impacts. Collectively, these factors lead to an overall significant enhancement of the traffic network. Using a variable speed limit (VSL) is one widely used SH technique explored in the literature. VSL involves changing the speed limit (generally reducing it) on a particular upstream of a bottleneck link. This is achieved using dynamic messages displayed on roadway signs for traditional vehicles, a suggested speed limit sent to connected vehicles (CVs), or by setting an imposed speed on connected and automated vehicles (CAVs). In this paper, VSL and SH are used interchangeably.

Ghiasi *et al.*'s [2] optimization approach used mixed traffic—human driven vehicles, CVs, and CAVs. They took a four step approach. First, an update collects information from road sensors and probe vehicles at every time step. Second, future downstream queues are predicted. Third, CAV trajectories are computed. Fourth, the authors use a shooting

The associate editor coordinating the review of this manuscript and approving it for publication was Zhe Xiao.

heuristic step, dividing the computed trajectory into four parabolic sections—deceleration, stopping, acceleration, and cruising—to prevent jumps in CAV trajectories. This methodology improved speed variations, throughput, surrogate safety measures, and fuel consumption, but it is also computationally expensive, as it has many steps, each requiring a great deal of calculation. The authors also assume advanced knowledge of the bottleneck location, around which a set of traffic sensors are deployed, which is not always possible in real world applications. Though the authors' model considers a one-lane roadway, it could be extended to a multi-lane scenario. Further details about SH strategies can be found in Ma *et al.*'s review [3], which lists research efforts in traditional SH and in SH with emerging technologies (CAVs).

SH techniques can be divided into two main categories: reactive and proactive (i.e., RSH and PSH). The RSH approach is activated after a set threshold (i.e., when congestion at a bottleneck starts to build up), and has been proven to be successful. Different control approaches have been used to solve the VSL problem. Jin *et al.* used a proportional-integral to prove VSL's effectiveness in increasing bottleneck discharge rate [4]. However, the authors used a kinematic wave model, which does not account for the stochastic nature of traffic. Yang *et al.* studied dynamic SH's impact on a lane drop bottleneck using a bang-bang feedback control [5]. However, they tested their method on a simple freeway section; additional testing on larger real networks with multiple SH zones is needed. Malikopoulos *et al.* developed an analytic solution for the optimal control problem applicable in real time [6], [7], which was also tested on a simple freeway section. In order to implement this method in real networks, some of the authors' assumptions need to be relaxed. In particular, lane changing and mixed traffic (human vehicles and CAVs) should be considered. Different optimization objectives are used in optimal control problems. Yang *et al.* implemented a tri-objective bi-level programming model intended to improve safety and reduce congestion and emissions [8]. Their model is effective but not suitable for dynamic conditions, as it was solved statically using a genetic algorithm.

Unlike RSH, PSH performs a traffic flow estimation before congestion occurs, then the SH algorithm is activated based on this estimation [6]. Yang *et al.* used a Kalman filter to estimate traffic states, then used optimal control to implement VSL [9]. Results were good, but the simulation was conducted for a simple freeway segment, with two on-ramps and one off-ramp, on which two VSL signs and seven detectors were installed. Future studies should consider a larger test network and selection of the optimal detector locations. Mittal *et al.* used a traffic estimation and prediction system relying exclusively on a mesoscopic simulator to estimate traffic conditions [10]; such models provide limited traffic operations details [11]. Many research efforts have combined control and estimation using Model Predictive Control (MPC) to predict and adjust vehicles' speeds as they move on the bottleneck's upstream link [12]–[14]. Each of the cited references had a different optimization objective, and some had multiple objectives. For instance, Khondaker and Kattan [13] tried to enhance mobility and safety while also fostering sustainability. Although MPC is popular, it has been demonstrated to be either costly to implement or sub-optimal. Frejo and Camacho [15], for example, showed that local MPC provides sub-optimal solutions and that global MPC is complicated to implement in real time. In addition, using MPC methods requires adequate state prediction accuracy, which is difficult when capacity drop-induced nonlinearity occurs. It is also important to note that most VSL research efforts have focused on small freeway sections [2], [10], [16].

On the network level, Tajalli and Hajbabaie [14] used constraints and linearized models in applying dynamic SH in urban street networks. The authors transformed the nonlinear model to a linear model to reduce system complexity, and found dynamic optimal advisory speed limits for the case study network. However, determining real-time solutions will be increasingly difficult as the size of the network grows. Yang *et al.* [8] tested their optimal control-based model on a Beijing network using a static genetic algorithm-based solution. Wang [17] used a macroscopic model to study the SH's network-wide impacts—i.e., the effects on transport efficiency and equity among different road users. Since Wang's model is macroscopic, it does not consider detailed vehicle interactions. In addition, the model used a small network with 7 nodes and 11 links; larger realistic networks should be considered. To the authors' knowledge, network-wide impact has never been studied extensively. Other limitations include the assumptions that bottleneck locations are fixed, and the data is gathered from fixed sensors installed on these bottlenecks [5]. Accordingly, tests on small freeway stretches might have unintended consequences. VSL could increase the bottleneck's discharge rate; however, this may also lead to a vehicle slowdown upstream of the bottleneck, which may create congestion on other parts of the freeway or network.

Data must be collected for the VSL to properly function; this data could be from loop detectors or probe vehicles. Mittal *et al.*'s work [10] assumed real-time information would be collected from sensors across the entire corridor, which is costly to implement. Tajalli and Hajbabaie [14] used probe vehicles, with 100% CAV market penetration rate, using linearized models and constraints. Ghiasi *et al.* [2] predicted traffic states based on both fixed sensors and probe vehicles, which may be more realistic than the other examples (100% probes or 100% loop detectors), but determining these fixed sensors' optimal locations is essential and could be difficult.

Previous studies showed that the SH feedback controllers were designed via the linearization around the fundamental diagram's critical density, which could be affected by the discontinuity of the fundamental diagram due to the capacity drop. A robust control technique is needed to address system uncertainties and the issue of non-linearity. Sliding mode control (SMC), which has the strength of simple design, global stability, and robustness is employed in this work to address the aforementioned issues. SMC represents a

powerful and robust method more appropriate for systems with uncertainties like exogenous signal and measurement errors [18].

In this research, a VSL or SH controller is developed using SMC to dynamically identify bottlenecks and then regulate CV speeds to disperse traffic congestion. Other previous work identified bottlenecks and locations of control a priori. This work extends the concept by identifying, in real-time, bottlenecks, control locations, and strategies. SMC is a non-linear control that alters the system dynamics by applying strong control actions when the system deviates from the desired behavior [19], [20]. SMC's advantages include its simplicity, its robustness to system disturbances, that it does not require linearization (i.e., not necessary to simplify the system dynamics), and that there is no requirement for accurate modeling [21], [22]. Sliding mode has been applied in many fields—mechanical, robotics, electrical, control systems, chaos theory, network control, etc. SMC has been also applied in CAV platooning [23], ramp metering control [24], and traffic routing [25]. The proposed controller is unique in two ways: (1) the system identifies bottlenecks dynamically rather than a priori; and (2) it identifies how and where to regulate CV speeds upstream of identified bottlenecks to disperse traffic congestion.

The developed controller was implemented and evaluated on a calibrated network of downtown Los Angeles composed of multiple connected freeways and signalized arterials. Testing allowed a large-scale dynamic system evaluation. The controller was implemented in the INTEGRATION microscopic traffic assignment and simulation software [26], which replicates vehicle longitudinal motion using the Rakha–Pasumarthy–Adjerid collision-free car-following model (the RPA model) [27]. Vehicles' movements are constrained by a vehicle dynamics model described in [28]. The vehicle delay model estimates were validated in [29], while vehicle stop estimations were described and validated in [30]. Vehicle lateral motion is modeled using lane-changing models described in [31]. Vehicle emissions and fuel consumption are modeled using the VT-Micro model [32].

A decentralized phase split/cycle length controller was used to optimize all traffic signals in the network [33]. The SH controller operated on all freeway links (a total of 331 links), and its operation was compared to the base case with no SH control. The proposed controller is a dynamic and adaptable solution to morphing and location-changing bottlenecks. The controller was evaluated on a network level (including all freeways and signalized arterial roadways) and along the freeway. The contributions of this paper are as follows:

- Includes dynamic identification of freeway bottlenecks;
- Uses a simple SMC to apply the SH control algorithm;
- Problem formulation and solution are based on the space mean speed, as obtained from probe vehicles (CVs)—no road sensors are required;
- Developed methodology is dynamic and adaptable to network conditions (i.e., a priori knowledge of bottleneck locations not required);
- Impacts are studied on a large real world network of multiple connected freeways and signalized urban roads.

This paper is organized as follows. Section II describes the nonlinear model and the proposed controller. Section III presents the experimental setup and results. Section IV provides a summary and concluding remarks.

II. PROPOSED MODEL AND CONTROLLER FORMULATION

A. MODEL FORMULATION

This section presents the SH controller's developed governing equations. The intent of the controller is to maintain a set average space mean speed on the network links. For a given link l (Figure 1), the time rate of density change, assuming no disturbance flow, is given by Equation 1.

$$\frac{dk_l(t)}{dt} = \frac{q_{in,l}(t)}{L_l} - \frac{q_{out,l}(t)}{L_l} \tag{1}$$

where, k_l is the density (i.e., number of vehicles per unit length on the link l), L_l is the length of link l, $q_{in,l}$ is the inflow of vehicles into the link l, and $q_{out,l}$ is the outflow of vehicles from the link.

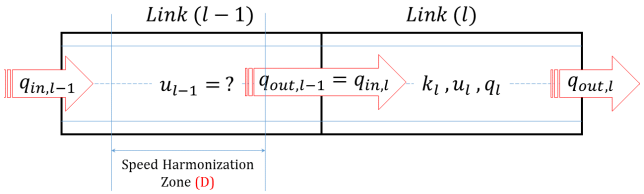

FIGURE 1. Two subsequent links: Link $l-1$ is feeding into link l.

Using the Van Aerde fundamental diagram [34], the density k_l can be expressed as a function of the link parameters and the current space mean speed on the link (Equation 2). It should be noted that the logic works with any fundamental diagram by replacing Equation 2 with the equation of the desired fundamental diagram.

$$k_l(t) = \frac{1}{c_1 + \frac{c_2}{u_{f,l} - u_l(t)} + c_3\, u_l(t)} \tag{2}$$

where $u_{f,l}$ is the free flow velocity on link l, $u_l(t)$ is the current space mean speed of vehicles on link l at time t, and the constants c_1, c_2, c_3 [34] are expressed below:

$$c_1 = \frac{u_{f,l}}{k_{j,l}\, {u_{c,l}}^2}\left(2\, {u_{c,l}}^2 - u_{f,l}\right)$$

$$c_2 = \frac{u_{f,l}}{k_{j,l}\, {u_{c,l}}^2}\left({u_{c,l}}^2 - u_{f,l}\right)^2$$

$$c_3 = \frac{1}{q_c} - \frac{u_{f,l}}{k_{j,l}\, {u_{c,l}}^2}$$

Using Equation 2, the density time rate of change k_l is given by Equation 3.

$$\frac{dk_l(t)}{dt} = \alpha\left(u_l(t)\right)\frac{du_l(t)}{dt}$$

where

$$\alpha(u_l(t)) = \frac{-c_2 - c_3\left(u_{f,l} - u_l(t)\right)^2}{\left(u_{f,l} - u_l(t)\right)^2\left(c_1 + \frac{c_2}{u_{f,l} - u_l(t)} + c_3\, u_l(t)\right)^2} \tag{3}$$

To find the system state equation ($\frac{du_l(t)}{dt}$), two assumptions were made [35], [36]: (1) the outflow of link l is proportional to the average flow on link l, and (2) the inflow into link l is equal to the outflow of link $l-1$. These assumptions are expressed in Equations 4 and 5.

$$q_{out,l}(t) = A.q_l(t) = A.k_l(t).u_l(t), \ \ where\ 0 \le A \le 1 \tag{4}$$

$$\begin{aligned} q_{in,l}(t) &= q_{out,l-1}(t) = A.q_{l-1}(t) \\ &= A.k_{l-1}(t).u_{l-1}(t) = A.k_{l-1}(t).u_{in}(t) \end{aligned} \tag{5}$$

Noting that $u_{l-1}(t)$ was labeled $u_{in}(t)$ (i.e., $u_{l-1}(t) = u_{in}(t)$), which will be considered as an input to the system at a later stage.

Using Equations 1, 3, 4 and 5, Equation 1 can be re-written as shown in Equations 6 and 7.

$$\begin{aligned} L_l.\alpha(u_l(t))\frac{du_l(t)}{dt} &= q_{in,l}(t) - q_{out,l}(t) \\ &= A.k_{l-1}(t).u_{in}(t) - A.k_l(t).u_l(t) \end{aligned} \tag{6}$$

$$\frac{du_l(t)}{dt} = -\frac{A.k_l(t)}{\alpha(u_l(t))\,L_l}.u_l(t) + \frac{A.k_{l-1}(t)}{\alpha(u_l(t))\,L_l}.u_{in}(t) \tag{7}$$

Assuming that

$$f(u_l(t)) = -\frac{A.k_l(t)}{\alpha(u_l(t))\,L_l}.u_l(t) \quad and \quad g(u_l(t)) = \frac{A.k_{l-1}(t)}{\alpha(u_l(t))\,L_l}$$

An ordinary differential equation governing the space mean speed time rate of change (u_l) on the link l with respect to an input u_{in} (i.e., the space mean speed of vehicles in the link $l-1$) is shown in Equation 8.

$$\frac{du_l(t)}{dt} = f(u_l(t)) \ + \ g\,(u_l(t))\ u_{in}(t) \tag{8}$$

The controller uses the nonlinear state equation (Equation 8) (as described in following subsection) to determine appropriate vehicle speeds (u_{in}) in the speed harmonization zone (Figure 1), so that the downstream link vehicle speeds (u_l) are regulated at the speed of capacity.

B. CONTROLLER FORMULATION

This section presents a controller design that regulates vehicle speeds in the speed harmonization zone (Figure 1) to maintain downstreak link vehicle speeds at the speed of capacity, using a SMC.

The system block diagram is shown in Figure 2 with an objective to control vehicle speeds (u_{in}) in the speed harmonization zone on link $l-1$ (Figure 1) so that the vehicles' space mean speed (u_l) on the downstream link l are regulated at a specific set-point; i.e., the speed at capacity ($\bar{u}_l$). Feedback speed (u_l) can be measured using CV-provided information, and can be estimated if not all vehicles are CVs. The advisory speed (u_{in}) can be displayed as a dynamic message on roadway signs, and/or sent to CVs. This study assumes that all vehicles are CVs.

SMC's central idea is to apply a control action when the system deviates from its desired behavior. The controller is capable of changing its structure; it can switch from one state to another at any time, and doesn't require accurate mathematical dynamic system modeling. SMC shows good performance when modeling uncertainties are present [37].

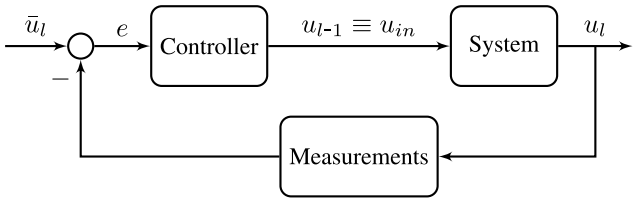

FIGURE 2. Speed harmonization system.

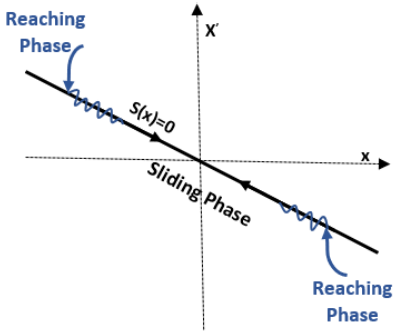

FIGURE 3. Phase plane plot of sliding control system.

SMC design involves two steps. (1) Designing the sliding surface that ensures stability of motion towards the coordinates' origin; this is called the existence problem (sliding phase in Figure 3). (2) Designing discontinuous control functions with appropriate switching logic to drive the system state from an arbitrary initial condition to the sliding surface, where it continues towards the origin; this is called the reachability problem (reaching phase in Figure 3).

The first step in designing is to choose a sliding (switching) surface (S), ensuring stability of motion, upon which the system is expected to converge and then remain [38]. The sliding surface is described below:

$$S(t) = u_l(t) - \bar{u}_l = 0 \tag{9}$$

This sliding motion occurs when the state reaches the sliding surface ($S(t) = 0$). The control that steps the state along the sliding surface is referred to as the equivalent control (u_{eq}), where the sliding motion dynamics are governed by $\dot{S}(t) = 0$ (i.e., necessary condition for sliding mode existence). Solving $\dot{S}(t) = \dot{u}_l(t) = 0$ for the control input ($u_{in}(t) = u_{eq}(t)$) yields:

$$\begin{aligned} u_{eq}(t) &= -g\,(u_l(t))^{-1} f\,(u_l(t)) \\ &= -\frac{\alpha\,(u_l(t))\ L_l}{A.k_{l-1}(t)}.\frac{-A.k_l(t).u_l(t)}{\alpha(u_l(t))\,L_l} = \frac{k_l(t)}{k_{l-1}(t)}u_l(t) \end{aligned} \tag{10}$$

Once the selection of a sliding surface with an appropriate control signal is complete, the second design step (reachability problem) involves selecting a state feedback control function, or hitting control, that can drive the state towards the surface and then maintain it there if the system initial conditions are not on S. The equivalent control is augmented with a discontinuous or switched control, as shown in Equation 11, where $u_{eq}(t)$ is a continuous control, $u_h(t)\ \ sign(S(t))$ is added to fulfill the reaching condition, where $sign(.)$ is the sign function.

$$u_{in}(t) = u_{eq}(t) - u_h(t)\ sign\,(S(t)) \tag{11}$$

The hitting control is responsible for pointing the system towards the sliding surface and depleting its energy (Lyapunov's second method [39]); this is translated through Equation 12, where η is a positive real number.

$$S(t)\ .\ \dot{S}(t) \leq -\eta\ |S(t)| \quad (12)$$

$$S(t)\ .\ [f(u_l(t)) + g(u_l(t))\ u_{in}(t)] \leq -\eta\ |S(t)| \quad (13)$$

namely,

$$S(t).[f(u_l(t)) + g(u_l(t)).(u_{eq}(t) - u_h(t)\ sign\ (S(t)))] \leq -\eta\ |S(t)| \quad (14)$$

which results in

$$u_h(t) \geq \eta g(u_l(t))^{-1} = \eta \frac{\alpha(u_l(t))\ L_l}{A.k_{l-1}(t)} \quad (15)$$

A convenient choice for $u_h(t)$ is given by Equation 16.

$$u_h(t) = \eta \frac{\alpha\ (u_l(t))\ L_l}{A.k_{l-1}(t)} \quad (16)$$

Substituting $u_{eq}(t)$ (Equation 10) and $u_h(t)$ (Equation 16) in Equation 11 yields Equation 17. $u_{in}(t)$ is expressed as a function of the density of the link in control (k_{l-1}), the density of the downstream link (k_l), and the velocity of the downstream link (u_l).

$$u_{in}(t) = \frac{k_l(t)}{k_{l-1}(t)}\ u_l(t) - \eta\ \frac{\alpha(u_l(t))\ L_l}{A\ k_{l-1}(t)}\ sign\ (u_l(t) - \bar{u}_l) \quad (17)$$

where $\alpha(u_l(t))$ is given by Equation 3.

For a discrete time step n, $u_{in}(n.\Delta t)$ is written as $u_{in}[n]$ (i.e., $u_{in}[n] = u_{in}(n.\Delta t)$, Equation 18), where Δt is the time step duration and is fixed a priori.

$$u_{in}[n] = \frac{k_l[n]}{k_{l-1}[n]} u_l[n] - \eta\ \frac{\alpha(u_l[n])\ L_l}{A\ k_{l-1}[n]}\ sign\ (u_l[n] - \bar{u}_l) \quad (18)$$

To maintain the vehicles' space mean speed on link l at the speed at capacity, vehicle speeds in the speed harmonization zone on the upstream link $(l-1)$ must follow Equation 18. To prevent the creation of artificial congestion on the upstream link $(l-1)$, we chose a localized application. The computed speed $u_{in}[n]$ will be enforced on a small specific region on link $(l-1)$. This region is referred to as the "speed harmonization zone", Figure 1, with a length D given by Equation 19.

$$D = min(d,\ \ R_d\ \times\ length(link\ l-1)) \quad (19)$$

where d is the maximum speed harmonization zone length, and R_d is the proportion of the link length that is allocated to the speed harmonization zone. Note that the speed harmonization zone is always centered at the middle of the link. This was based on experimentation with different locations, and the center was found to work best.

The SH controller is activated on the speed harmonization zone on the upstream link once the density on the downstream link is within a specific range, as outlined in the following equation:

$$R_{kmin} \times k_{j,l} \leq k_l \leq R_{kmax} \times k_{j,l} \quad (20)$$

where $k_{j,l}$ is the jam density on the link l and R_{kmin} and R_{kmax} are given parameters. The density (k_l) can be measured using information provided by CVs or estimated if not all vehicles are CVs [40], [41]. This activation condition ensures that the SH controller is only activated when the downstream link starts to become congested in order to avoid artificial congestion (needless reduction in vehicles' speeds) on the upstream link.

III. SIMULATION SETUP AND RESULTS

This section covers the simulation setup and results of a large scale real network study to control vehicle speed on freeway links using the SH controller in downtown Los Angeles, California.

A. SIMULATION SETUP

Microscopic simulations were conducted on a large network—an area of downtown LA, which is the most congested downtown area, as shown in Figure 4(a). There are 331 freeway links in this network, which are colored in red in Figure 4(b).

Network traffic signals are optimized by a decentralized phase split/cycle length controller [33]. The SH controller was applied only on freeways and its operation was compared to the base no-control case. Simulations were carried out using the calibrated morning peak hour traffic (7 : 00−8 : 00 a.m.). Vehicles were loaded for one hour; extra

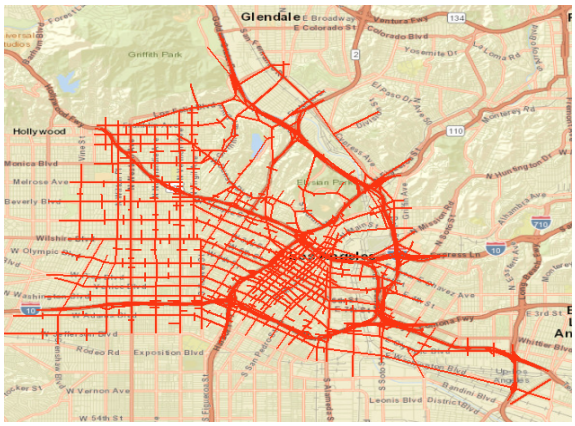

(a) LA, Google maps.

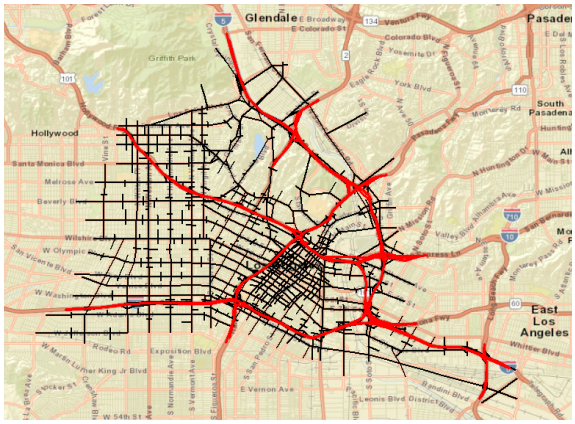

(b) LA Freeway, Google maps.

FIGURE 4. Downtown LA network.

time was given at the end of the simulation to make sure that all vehicles departed the network. This was to ensure an equal number of vehicles were in the network when comparing the operation of the proposed controller to the base case.

The downtown LA network shown in Figure 4(a) has 457 signalized intersections, 23 yield signs, 285 stop signs, and a total of 3,556 links, with 331 freeway links [42]. The origin-destination demand was calibrated based on vehicle count data from loop detectors [43] using QueensOD software [44] with 143,957 total trips. The phasing scheme for the intersections varied from 2 to 6 phases, which is consistent with the phases implemented in downtown LA. The minimum network link length was 50 m, and the maximum was 4,400 m. The network minimum free-flow speed was 15 (km/h), and the maximum was 120 (km/h). The links' jam density was 180 ($veh/km/lane$).

The INTEGRATION microscopic software, which traces individual vehicle movements every deci-second, was used to evaluate the proposed controller's performance [26], [45]. INTEGRATION was used for a number of reasons, one of which is that, through it's unique car-following modeling, it captures the capacity drop associated with the onset of congestion. This phenomenon has been validated against empirical data [46]. Furthermore, the lane-changing logic has been validated against empirical data [31]. Examples of stochastic variables integrated in the software include driver specifications such as acceleration/deceleration rates, reaction times, desired speeds, and lane-changing behavior. The following measures of effectiveness (MOEs) were measured to assess the system's operation:

- Average Travel Time (s/veh): aggregated trip times divided by the total number of vehicles.
- Average Total Delay (s/veh): aggregated vehicle delay (i.e., the sum of the difference in travel time between travelling at instantaneous vehicle speed and travelling at the free-flow speed) divided by the total number of vehicles.
- Average Stopped Delay (s/veh): the sum of instances where vehicle speed is less than or equal to pedestrian speed (3.6 (km/h)) divided by the total number of vehicles.
- Average Queue Length (veh): aggregated vehicles in queue each second divided by the simulation time.
- Average Fuel (L/veh): aggregated fuel consumed by vehicles divided by the total number of vehicles.
- Average CO2 (grams/veh): aggregated CO2 produced divided by the total number of vehicles.

B. SIMULATION SCENARIOS

Several simulations with different control parameter values were implemented to study their effect on the proposed SH freeway controller's performance; however, only three scenarios (SH-1, SH-2, SH-3) are described below, with $\Delta t = 3\ s, \eta = 1, R_{kmin} = 0.5, R_{kmax} = 0.9$:

$$SH-1 \Rightarrow R_d = 0.1, d = 10\ m, A = 1$$
$$SH-2 \Rightarrow R_d = 0.06, d = 6\ m, A = 0.8$$
$$SH-3 \Rightarrow R_d = 0.04, d = 4\ m, A = 1$$

1) IMPACT OF THE TIME STEP (Δt)

Extensive sensitivity analyses revealed that with an increasing time step (Δt), recommended vehicle velocities (u_{in}) in the control zone will not be updated frequently, and might be out of phase with the dynamic changes on the downstream link. On the other hand, decreasing (Δt) will result in short vehicle time intervals to receive and apply the recommended speed. Vehicles in the control zone may also update their speeds multiple times, possibly creating turbulence and raising safety issues.

2) EFFECTS OF THE CONTROL ZONE LENGTH (D)

The sensitivity analysis showed that an increasing control zone length (D, Figure 1) led to more vehicles in that zone and consequently more vehicles adopting the recommended speed. This, in turn, might cause artificial congestion (needless reduction in vehicles' speeds) on the upstream link. In contrast, a decreased control zone length led to not enough vehicles getting the chance to apply the controller recommendation to improve the system's performance.

3) ACTIVATION CONDITION IMPACT (R_{kmin} & R_{kmax})

The controller activation condition (Equation 20) ensures that the SH controller is only activated when the downstream link starts to become congested in order to avoid artificial congestion on the upstream link. Analyses showed that early controller activation results in artificial congestion, and late activation has no impact on the system's performance.

C. SIMULATION RESULTS AND DISCUSSION

The operation of the developed controller was evaluated at the network and freeway links level.

1) OVERALL NETWORK PERFORMANCE

The average MOE values over the entire network (Figure 4(a)) for the base case and for different SH controller scenarios are shown in Table 1, in addition to the percentage of improvement relative to the base case. The improvement (%) is calculated as:

$$Imp.(\%) = \frac{MOE(Base) - MOE(SH)}{MOE(Base)} \times 100 \qquad (21)$$

The simulation results (SH-3 scenario) show a significant reduction in average travel time (12.17%), average total delay (20.67%), average stopped delay (39.58%), average fuel consumption (2.6%), and average CO_2 emissions (3.3%).

2) FREEWAY PERFORMANCE

The LA network has 457 signalized intersections, 30 yield signs, and 459 stop signs where the SH controller is not activated, which might obfuscate the improvements shown with the proposed controller. To get a clearer picture of the SH controller's benefits, we evaluated the introduced logic's impact on the freeways only. In this case, the benchmark scenario will also involve freeways only, as shown in Figure 4(b).

TABLE 1. Network MOEs and improvement (%) using SH controller over base case.

MOE \ System	Base	SH-1	SH-2	SH-3
Average Travel Time (s/veh)	1034.27	944.36	932.03	908.37
Improvement %		8.69	9.88	12.17
Average Total Delay (s/veh)	557.46	476.22	466.46	442.25
Improvement %		14.57	16.32	20.67
Average Stopped Delay (s/veh)	256.77	170.41	162.47	155.13
Improvement %		33.63	36.72	39.58
Average Fuel (L/veh)	1.16	1.14	1.13	1.12
Improvement %		1.51	1.84	2.6
Average CO2 (grams/veh)	2482.13	2430.88	2421.67	2400.15
Improvement %		2.06	2.44	3.3

TABLE 2. Freeway links MOEs and improvement (%) using SH controller over base case.

MOE \ System	Base	SH-3	Imp. (%)
Average Travel Time (s/veh)	41.99	33.39	20.48
Average Queued Vehicles (veh/link)	17.09	13.39	21.63
Total Fuel Consumption (L/link)	297.29	289.67	2.56
Total CO_2 Emissions (grams/link)	615800	592710	3.75

Table 2 presents the MOEs' improvement percentage over the base case using the SH controller (SH-3 scenario). An average travel time reduction of 20.48% was achieved. Similarly, there was a reduction in the number of average queued vehicles per link, total fuel consumption per link, and total CO_2 emissions per link of 21.63%, 2.6%, and 3.75% respectively. These results indicate that the SH controller is so efficient on the freeway links that it impacts the total averages of the whole network.

IV. SUMMARY AND CONCLUSIONS

In this paper, a freeway speed harmonization controller that takes advantage of CVs was developed. The developed controller employs SMC theory coupled with VSL control to effectively reduce highway traffic congestion. The developed control logic was implemented and tested using the INTEGRATION microscopic traffic software in a graph of downtown Los Angeles, California that includes signalized arterials and freeways. The developed SH controller's operation, which was only employed on freeways, was compared to a base case control scenario. For both cases (base and highway), all signalized intersections operated using decentralized phase split/cycle length optimization controllers.

The results revealed that the developed controller led to significant improvements in network-wide (freeway and non-freeway links) measures of performance. In particular, the average travel time was reduced by 12.17%, as was total delay (by 20.67%), stopped delay (by 39.58%), and CO_2 emissions (by 3.3%) over the base case scenario with no freeway control. Furthermore, the results show substantial improvements in freeway operations, with a reduction in the average travel time of 20.48%, in queue length of 21.63%, in fuel consumption of 2.56%, and in CO_2 emissions of 3.75%.

The results show that the proposed SH controller has significant potential benefits when activated on highways on large scale networks. This controller makes efficient use of the current network infrastructure, increases highway traffic handling capacity, and reduces congestion. Future work will include testing the controller for different levels of CV market penetration levels.

REFERENCES

[1] M. I. Elbakary, H. M. Abdelghaffar, K. Afrifa, H. A. Rakha, M. Cetin, and K. M. Iftekharuddin, "Aerosol detection using lidar-based atmospheric profiling," *Proc. SPIE*, vol. 10395, Aug. 2017, Art. no. 103951H.

[2] A. Ghiasi, X. Li, and J. Ma, "A mixed traffic speed harmonization model with connected autonomous vehicles," *Transp. Res. C, Emerg. Technol.*, vol. 104, pp. 210–233, Jul. 2019.

[3] J. Ma, X. Li, S. Shladover, H. A. Rakha, X.-Y. Lu, R. Jagannathan, and D. J. Dailey, "Freeway speed harmonization," *IEEE Trans. Intell. Vehicles*, vol. 1, no. 1, pp. 78–89, Mar. 2016.

[4] H.-Y. Jin and W.-L. Jin, "Control of a lane-drop bottleneck through variable speed limits," *Transp. Res. C, Emerg. Technol.*, vol. 58, pp. 568–584, Sep. 2015.

[5] H. Yang and H. Rakha, "Feedback control speed harmonization algorithm: Methodology and preliminary testing," *Transp. Res. C, Emerg. Technol.*, vol. 81, pp. 209–226, Aug. 2017.

[6] A. A. Malikopoulos, S. Hong, B. B. Park, J. Lee, and S. Ryu, "Optimal control for speed harmonization of automated vehicles," *IEEE Trans. Intell. Transp. Syst.*, vol. 20, no. 7, pp. 2405–2417, Jul. 2019.

[7] S. Hong, A. A. Malikopoulos, B. B. Park, and J. Lee, "Speed harmonization using optimal control algorithm under mixed traffic of connected-automated and human driven vehicles," in *Proc. Transp. Res. Board 97th Annu. Meeting*, Washington, DC, USA, Jan. 2018, Paper 18-06228. [Online]. Available: https://trid.trb.org/view/1497173

[8] Y. Yang, H. Lu, Y. Yin, and H. Yang, "Optimization of variable speed limits for efficient, safe, and sustainable mobility," *Transp. Res. Rec., J. Transp. Res. Board*, vol. 2333, no. 1, pp. 37–45, Jan. 2013.

[9] X. Yang, Y. Lin, Y. Lu, and N. Zou, "Optimal variable speed limit control for real-time freeway congestions," *Procedia-Social Behav. Sci.*, vol. 96, pp. 2362–2372, Nov. 2013.

[10] A. Mittal, E. Kim, H. S. Mahmassani, and Z. Hong, "Predictive dynamic speed limit in a connected environment for a weather affected traffic network: A case study of Chicago," *Transp. Res. Rec., J. Transp. Res. Board*, vol. 2672, no. 19, pp. 13–24, Dec. 2018.

[11] W. Burghout, H. N. Koutsopoulos, and I. Andreasson, "A discrete-event mesoscopic traffic simulation model for hybrid traffic simulation," in *Proc. IEEE Intell. Transp. Syst. Conf.*, Sep. 2006, pp. 1102–1107.

[12] A. Hegyi, B. De Schutter, and J. Heelendoorn, "MPC-based optimal coordination of variable speed limits to suppress shock waves in freeway traffic," in *Proc. Amer. Control Conf.*, vol. 5, Jun. 2003, pp. 4083–4088.

[13] B. Khondaker and L. Kattan, "Variable speed limit: A microscopic analysis in a connected vehicle environment," *Transp. Res. C, Emerg. Technol.*, vol. 58, pp. 146–159, Sep. 2015.

[14] M. Tajalli and A. Hajbabaie, "Dynamic speed harmonization in connected urban street networks," *Comput.-Aided Civil Infrastruct. Eng.*, vol. 33, no. 6, pp. 510–523, Jun. 2018.

[15] J. R. D. Frejo and E. F. Camacho, "Global versus local MPC algorithms in freeway traffic control with ramp metering and variable speed limits," *IEEE Trans. Intell. Transp. Syst.*, vol. 13, no. 4, pp. 1556–1565, Dec. 2012.

[16] J. R. D. Frejo, I. Papamichail, M. Papageorgiou, and B. De Schutter, "Macroscopic modeling of variable speed limits on freeways," *Transp. Res. C, Emerg. Technol.*, vol. 100, pp. 15–33, Mar. 2019.

[17] S. Wang, "Efficiency and equity of speed limits in transportation networks," *Transp. Res. C, Emerg. Technol.*, vol. 32, pp. 61–75, Jul. 2013.

[18] V. I. Utkin, *Sliding Modes in Control and Optimization*. Berlin, Germany: Springer, 1992.

[19] J. Y. Hung, W. Gao, and J. C. Hung, "Variable structure control: A survey," *IEEE Trans. Ind. Electron.*, vol. 40, no. 1, pp. 2–22, Feb. 1993.

[20] C. Edwards and S. Spurgeon, *Sliding Mode Control: Theory and Applications*. Boca Raton, FL, USA: CRC Press, 1998.

[21] X. Zhao, H. Yang, W. Xia, and X. Wang, "Adaptive fuzzy hierarchical sliding-mode control for a class of MIMO nonlinear time-delay systems with input saturation," *IEEE Trans. Fuzzy Syst.*, vol. 25, no. 5, pp. 1062–1077, Oct. 2017.

[22] M. T. Hamayun, C. Edwards, and H. Alwi, *Fault Tolerant Control Schemes Using Integral Sliding Modes*. Cham, Switzerland: Springer, 2016. [Online]. Available: https://www.springer.com/gp/book/9783319322360
[23] A. Ferrara, R. Librino, A. Massola, M. Miglietta, and C. Vecchio, "Sliding mode control for urban vehicles platooning," in *Proc. IEEE Intell. Vehicles Symp.*, Jun. 2008, pp. 877–882.
[24] V. Dryankova, H. Abouaïssa, D. Jolly, and H. Haj-Salem, "Traffic network ramp metering based on High Order Sliding Mode and flatness approaches: A case study," in *Proc. 4th Int. Conf. Logistics*, May/Jun. 2011, pp. 274–280.
[25] H. Majid, C. Lu, and H. Karim, "An integrated approach for dynamic traffic routing and ramp metering using sliding mode control," *J. Traffic Transp. Eng. (English Ed.)*, vol. 5, no. 2, pp. 116–128, Apr. 2018.
[26] H. A. Rakha, "Integration release 2.40 for windows: User's guide–Volume II: Advanced model features," Center Sustain. Mobility, Virginia Tech Transp. Inst., Blacksburg, VA, USA, Tech. Rep., Jun. 2013.
[27] H. Rakha, P. Pasumarthy, and S. Adjerid, "A simplified behavioral vehicle longitudinal motion model," *Transp. Lett.*, vol. 1, no. 2, pp. 95–110, Apr. 2009.
[28] H. A. Rakha, M. Snare, and F. Dion, "Vehicle dynamics model for estimating maximum light duty vehicle acceleration levels," *Transp. Res. Rec., J. Transp. Res. Board*, vol. 1883, nos. 40–49, 2004.
[29] F. Dion, H. Rakha, and Y.-S. Kang, "Comparison of delay estimates at under-saturated and over-saturated pre-timed signalized intersections," *Transp. Res. B, Methodol.*, vol. 38, no. 2, pp. 99–122, Feb. 2004.
[30] H. Rakha, Y.-S. Kang, and F. Dion, "Estimating vehicle stops at undersaturated and oversaturated fixed-time signalized intersections," *Transp. Res. Rec., J. Transp. Res. Board*, vol. 1776, no. 1, pp. 128–137, Jan. 2001.
[31] H. A. Rakha and Y. Zhang, "INTEGRATION 2.30 framework for modeling lane-changing behavior in weaving sections," *Transp. Res. Rec., J. Transp. Res. Board*, vol. 1883, no. 1, pp. 140–149, 2004.
[32] H. A. Rakha, K. Ahn, and A. Trani, "Development of VT-Micro model for estimating hot stabilized light duty vehicle and truck emissions," *Transp. Res. D, Transp. Environ.*, vol. 9, no. 1, pp. 49–74, 2004.
[33] R. Roess, E. S. Prassas, and W. R. McShane, *Traffic Engineering*, 4th ed. Upper Saddle River, NJ, USA: Pearson Higher Education, 2010.
[34] H. Rakha, "Validation of van Aerde's simplified steadystate car-following and traffic stream model," *Transp. Lett.*, vol. 1, no. 3, pp. 227–244, Jul. 2009.
[35] M. Keyvan-Ekbatani, A. Kouvelas, I. Papamichail, and M. Papageorgiou, "Exploiting the fundamental diagram of urban networks for feedback-based gating," *Transp. Res. B, Methodol.*, vol. 46, no. 10, pp. 1393–1403, Dec. 2012.
[36] M. Elouni and H. Rakha, "Weather-tuned network perimeter control-a network fundamental diagram feedback controller approach," in *Proc. VEHITS*, 2018, pp. 82–90.
[37] Y. Shtessel, C. Edwards, L. Fridman, and A. Levant, *Sliding Mode Control and Observation*. New York, NY, USA: Springer, 2014. [Online]. Available: https://www.springer.com/gp/book/9780817648923
[38] K. R. Buckholtz, "Reference input wheel slip tracking using sliding mode control," in *Proc. SAE Tech. Paper Ser.*, Mar. 2002, pp. 477–483.
[39] A. T. Azar and Q. Zhu, *Advances and Applications in Sliding Mode Control Systems*. Cham, Switzerland: Springer, 2015. [Online]. Available: https://www.springer.com/gp/book/9783319111728
[40] M. A. Aljamal, H. M. Abdelghaffar, and H. A. Rakha, "Developing a neural–Kalman filtering approach for estimating traffic stream density using probe vehicle data," *Sensors*, vol. 19, no. 19, p. 4325, 2019.
[41] M. A. Aljamal, H. M. Abdelghaffar, and H. A. Rakha, "Real-time estimation of vehicle counts on signalized intersection approaches using probe vehicle data," *IEEE Trans. Intell. Transp. Syst.*, early access, Feb. 21, 2020, doi: 10.1109/TITS.2020.2973954.
[42] H. M. Abdelghaffar and H. A. Rakha, "A novel decentralized game-theoretic adaptive traffic signal controller: Large-scale testing," *Sensors*, vol. 19, no. 10, p. 2282, May 2019.
[43] J. Du, H. A. Rakha, A. Elbery, and M. Klenk, "Microscopic simulation and calibration of a large-scale metropolitan network: Issues and proposed solutions," in *Proc. Transp. Res. Board 97th Annu. Meeting*, Washington, DC, USA, Jan. 2018, Paper 18-02086. [Online]. Available: https://trid.trb.org/view/1495169
[44] M. V. Aerde and H. A. Rakha, "Queensod rel. 2.10-user's guide: Estimating origin-destination traffic demands from link flow counts," Center Sustain. Mobility, Virginia Tech Transp. Inst., Blacksburg, VA, USA, Tech. Rep., Mar. 2010.
[45] H. A. Rakha, "Integration release 2.40 for windows: User's guide—Volume I: Fundamental model features," Center Sustain. Mobility, Virginia Tech Transp. Inst., Blacksburg, VA, USA, Tech. Rep., Oct. 2012.
[46] E. Chamberlayne, H. Rakha, and D. Bish, "Modeling the capacity drop phenomenon at freeway bottlenecks using the INTEGRATION software," *Transp. Lett.*, vol. 4, no. 4, pp. 227–242, Oct. 2012.

HOSSAM M. ABDELGHAFFAR received the B.Sc. degree (Hons.) in electronics engineering from the Faculty of Engineering, Mansoura University, Egypt, the M.Sc. degree in automatic control system engineering from Mansoura University, and the Ph.D. degree in electrical engineering from the Bradley Department of Electrical and Computer Engineering, Virginia Tech, USA. He is currently an Assistant Professor with the Department of Computer Engineering and Systems, Faculty of Engineering, Mansoura University, and the Center for Sustainable Mobility, Virginia Tech Transportation Institute, Virginia Tech.

MAHA ELOUNI received the B.Sc. and M.Sc. degrees in computer science from the National School of Computer Science, Tunisia, in 2012, and the M.Sc. degree in applied mathematics from Virginia Tech, in 2015. She is currently pursuing the Ph.D. degree with the Bradley Department of Electrical and Computer Engineering, Virginia Tech. She works as a Graduate Research Assistant with the Center for Sustainable Mobility, Virginia Tech Transportation Institute. Her research interests include traffic control, traffic modeling and simulation, and intelligent transportation systems.

YOUSSEF BICHIOU received the B.Sc. degree from the Department of Mechanical Engineering, Tunisia Polytechnic School, La Marsa, Tunisia, and the Ph.D. degree in engineering mechanics from the Virginia Polytechnic Institute and State University (Virginia Tech). He is currently a Research Associate with the Center for Sustainable Mobility, Virginia Tech Transportation Institute, Blacksburg, VA, USA. His research interests include traffic flow theory, autonomous vehicle control, traffic congestion alleviation, and intersection control.

HESHAM A. RAKHA (Fellow, IEEE) received the B.Sc. degree (Hons.) in civil engineering from Cairo University, Cairo, Egypt, in 1987, and the M.Sc. and Ph.D. degrees in civil and environmental engineering from Queen's University, Kingston, ON, Canada, in 1990 and 1993, respectively. He and his team have developed a suite of multimodal agent-based transportation modeling tools, including the INTEGRATION microscopic traffic simulation software. This software was used to evaluate the first dynamic route guidance system, TravTek, Orlando, FL; to model the Greater Salt Lake City area in preparation for the 2002 Winter Olympic Games; to model sections of Beijing in preparation for the 2008 Summer Olympic Games; to optimize and evaluate the performance of alternative traveler incentive strategies to reduce network-wide energy consumption in the Greater Los Angeles area; and to develop and test an Eco-Cooperative Automated Control (Eco-CAC) System. Finally, he and his team have developed various vehicle energy and fuel consumption models that are used world-wide to assess the energy and environmental impacts of ITS applications and emerging connected automated vehicle (CAV) systems. He is currently a Professional Engineer in Ontario, Canada. His research interests include large-scale transportation system optimization, modeling, and assessment. He serves as an Editor and an Associate Editor on a number of journals, including the IEEE TRANSACTIONS ON INTELLIGENT TRANSPORTATION SYSTEMS.